Supporting Information

Residue-Driven Degradation and Its Stabilization in NaCl-Assisted WS_2 with 3R Stacking Enrichment

Lia Saptini Handriani[1], *Hyeonsu Park*[1], *Zhe Gao*[1], *Jae-il Jang*[1], *and Won Il Park*[1]*

[1]Division of Materials Science and Engineering, Hanyang University, Seoul, 04763, Republic of Korea

*Email: wipark@hanyang.ac.kr1

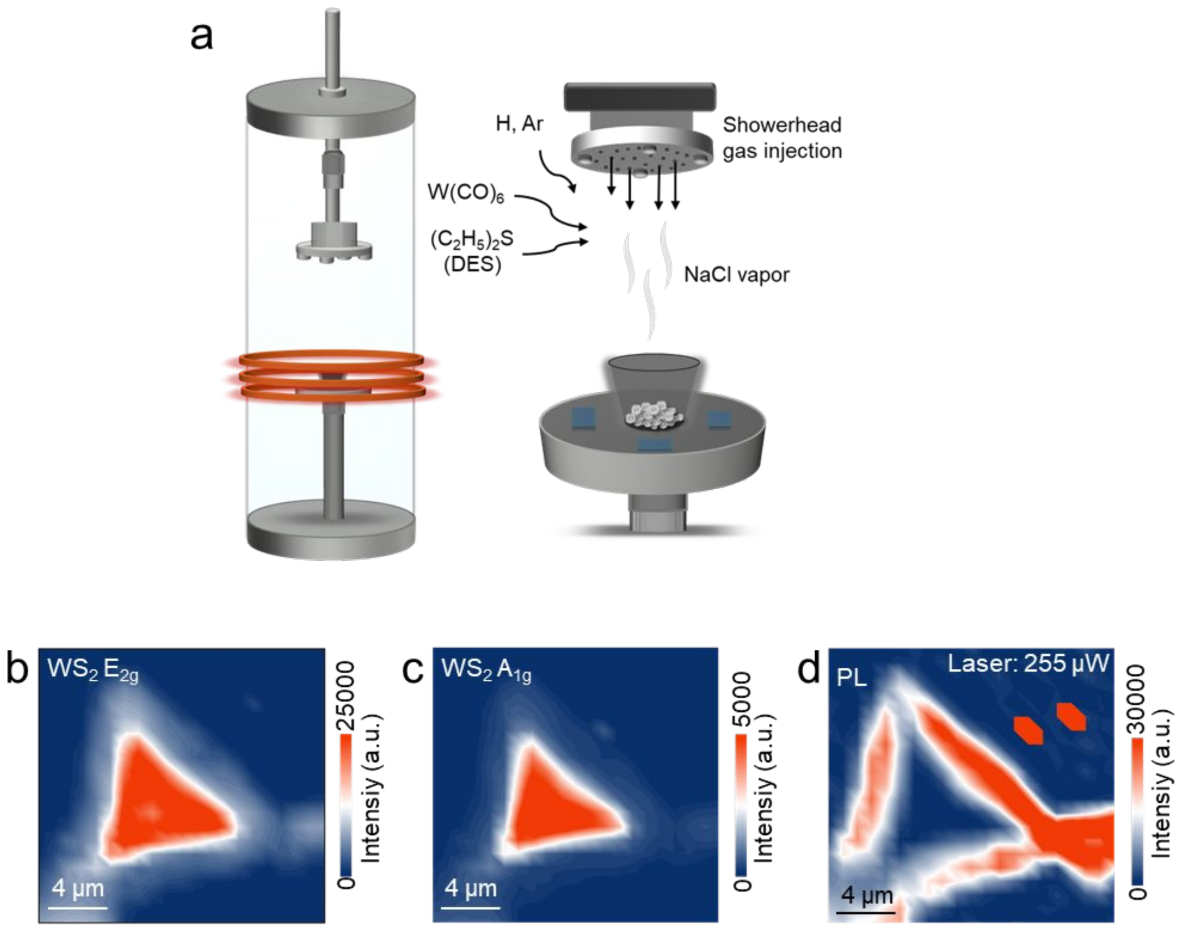

Figure S1. (a) Schematic of the vertical MOCVD process used for NaCl-assisted WS_2 growth on SiO_2/Si. (b,c) Raman E_{2g} and A_{1g} intensity maps of a representative as-grown triangular WS_2 flake. (d) PL intensity map of the same flake.

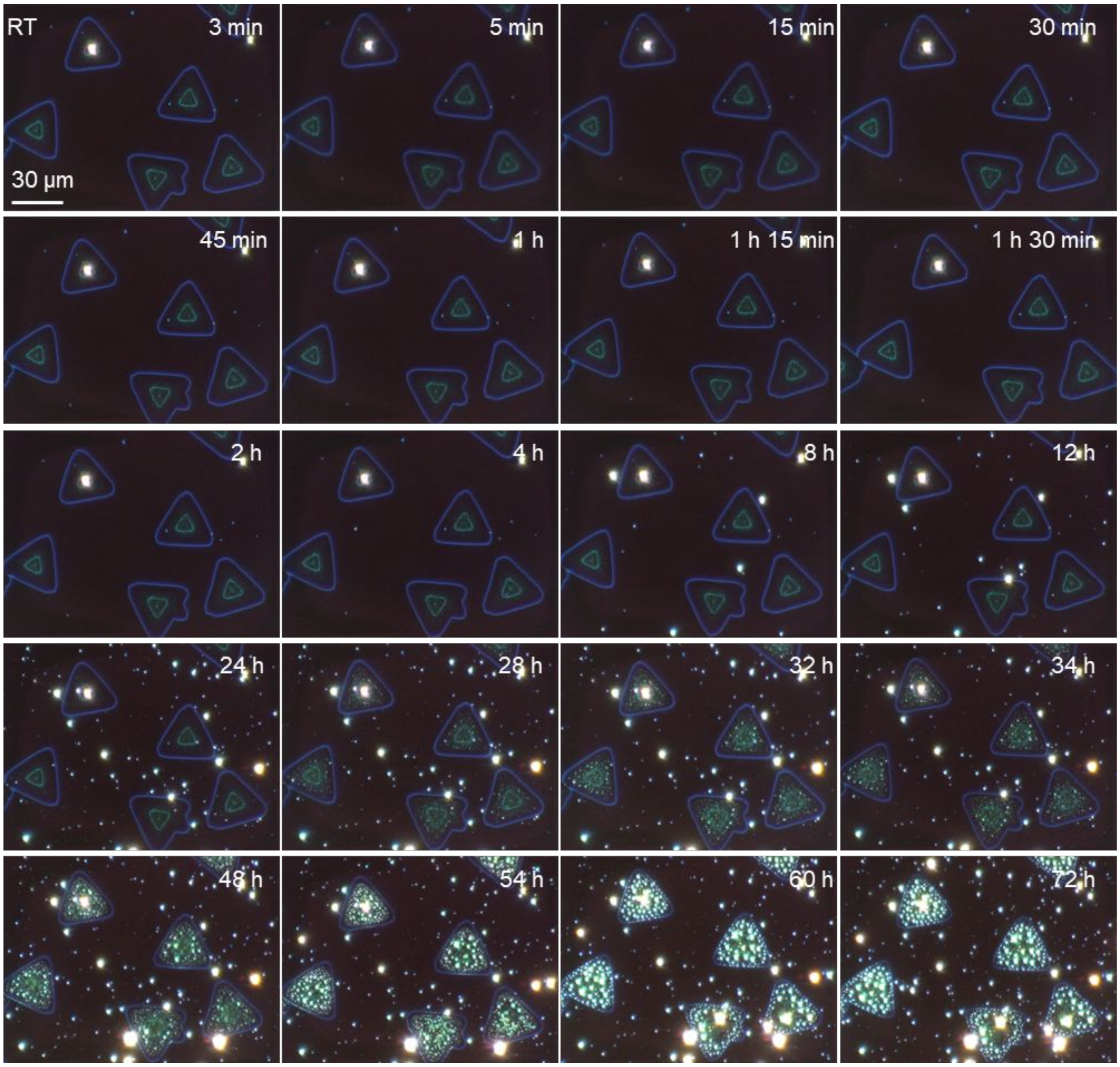

Figure S2. (a) Dark-field optical microscopy images of representative as-grown WS_2 flakes recorded during ambient air exposure from 3 min to 72 h.

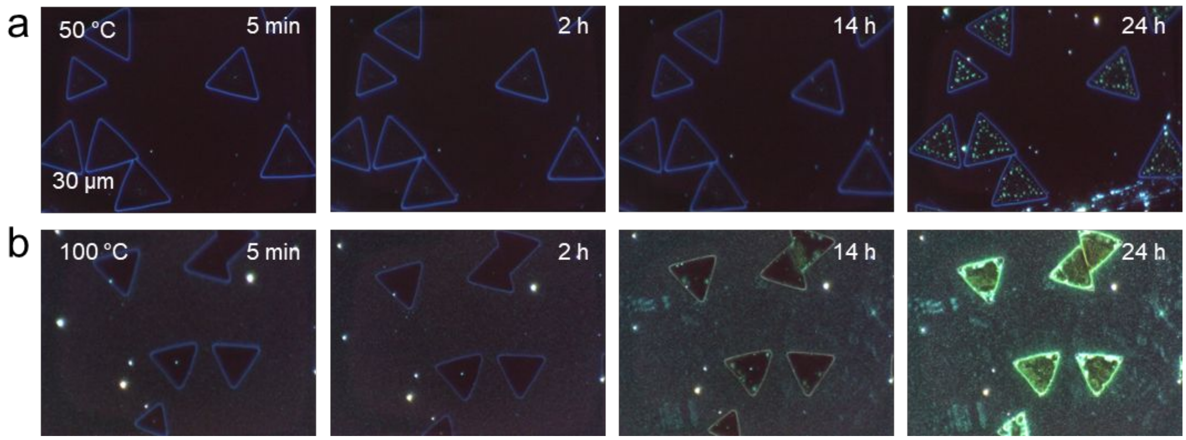

Figure S3. (a–b) Dark-field optical microscopy images of as-grown NaCl-assisted WS_2 recorded during ambient air exposure at 50 ˚C and 100 ˚C, respectively, showing the time-dependent degradation at elevated exposure temperatures.

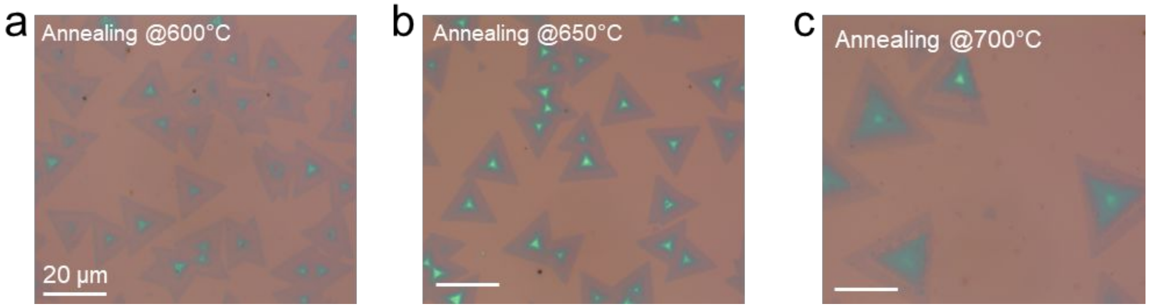

Figure S4. (a–c) Optical microscopy images of representative NaCl-assisted WS_2 flakes after PGA at 600, 650, and 700 ˚C, respectively, under otherwise identical sulfur-rich conditions, imaged after 1 day of ambient air exposure. The 650 ˚C condition (b) retains a well-defined triangular morphology after exposure, whereas residual post-exposure damage remains at 600 ˚C (a) and thermally induced morphological degradation is observed at 700 ˚C (c).

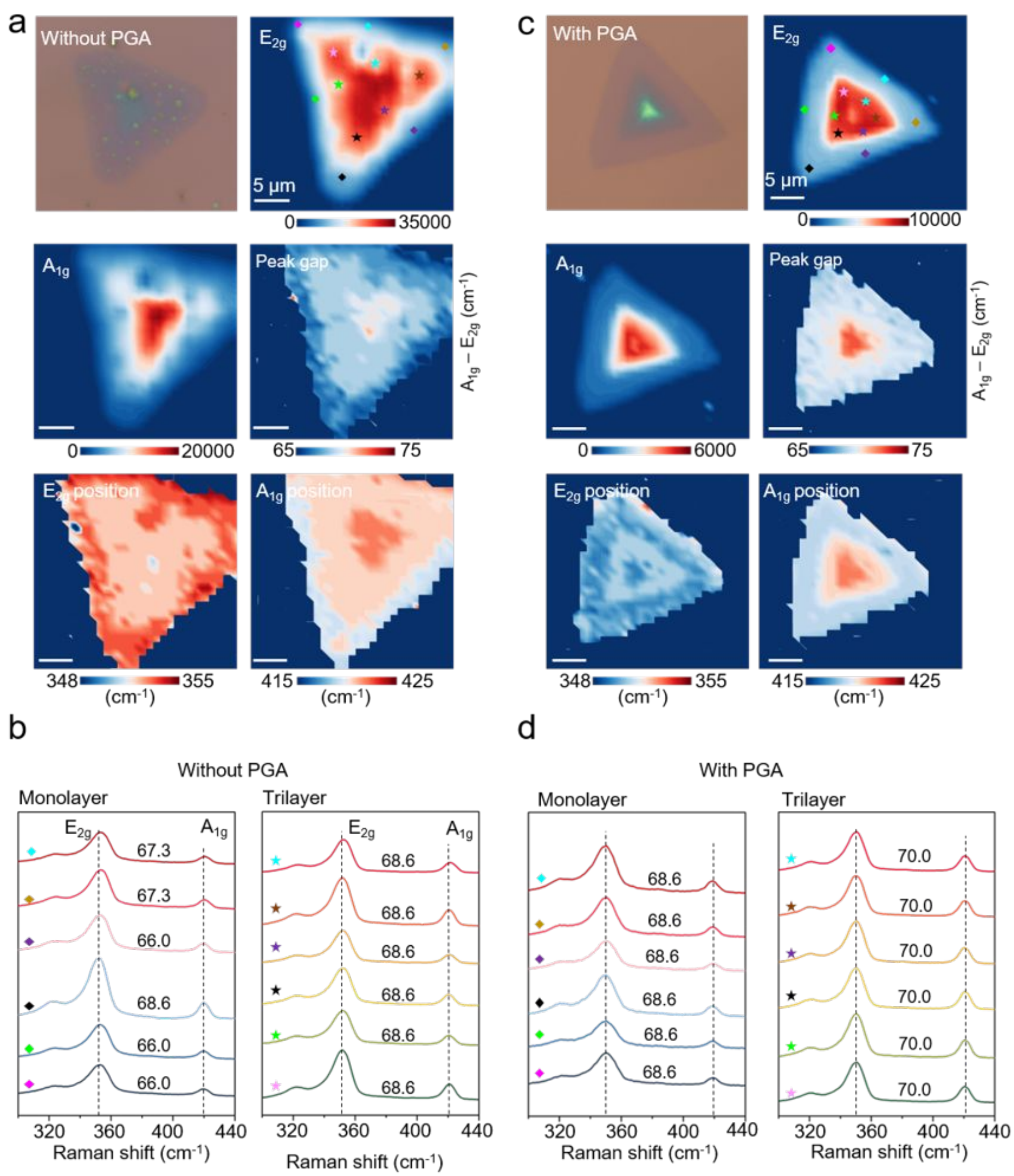

Figure S5. Spatially-resolved Raman analysis of NaCl-assisted WS_2 before and after PGA. (a) Optical microscopy image and corresponding E_{2g} intensity, A_{1g} intensity, peak gap $\Delta\omega = \omega_{A_{1g}} - \omega_{E_{2g}}$, E_{2g} position, and A_{1g} position maps without PGA. (b) Representative Raman point spectra from monolayer and trilayer positions marked in panel a. (c) Corresponding maps of PGA-treated WS_2 with identical layout to panel a. (d) Representative Raman point spectra from monolayer and trilayer positions marked in panel c. Colored symbols correspond to sampling positions in the respective E_{2g} intensity maps.

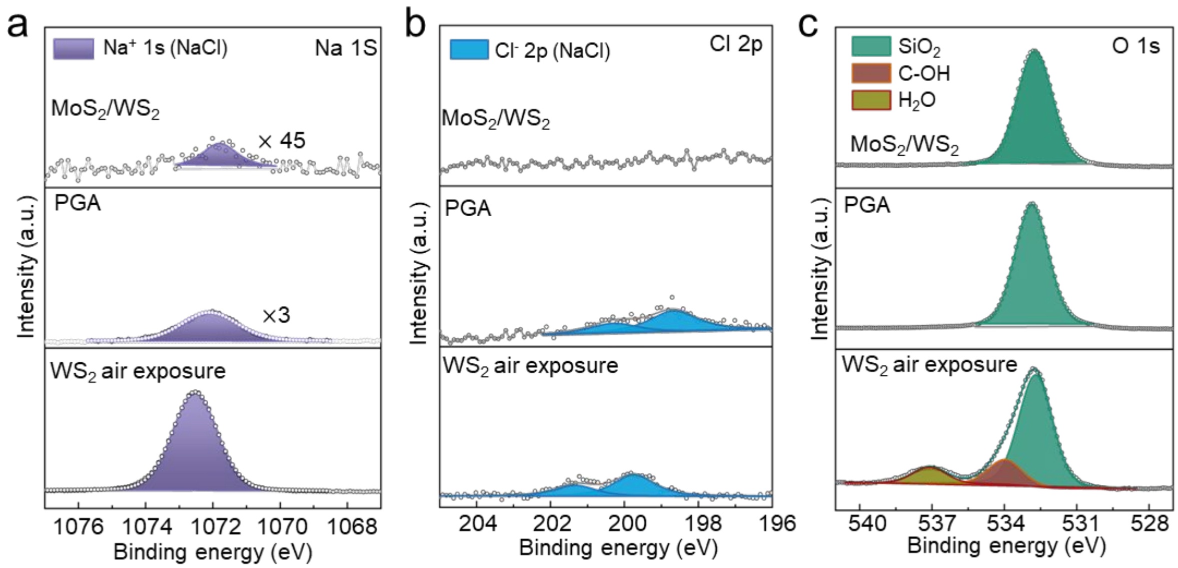

Figure S6. (a) Na 1s, (b) Cl 2p, and (c) O 1s XPS spectra of air-exposed, PGA-treated, and MoS_2-capped WS_2 samples.

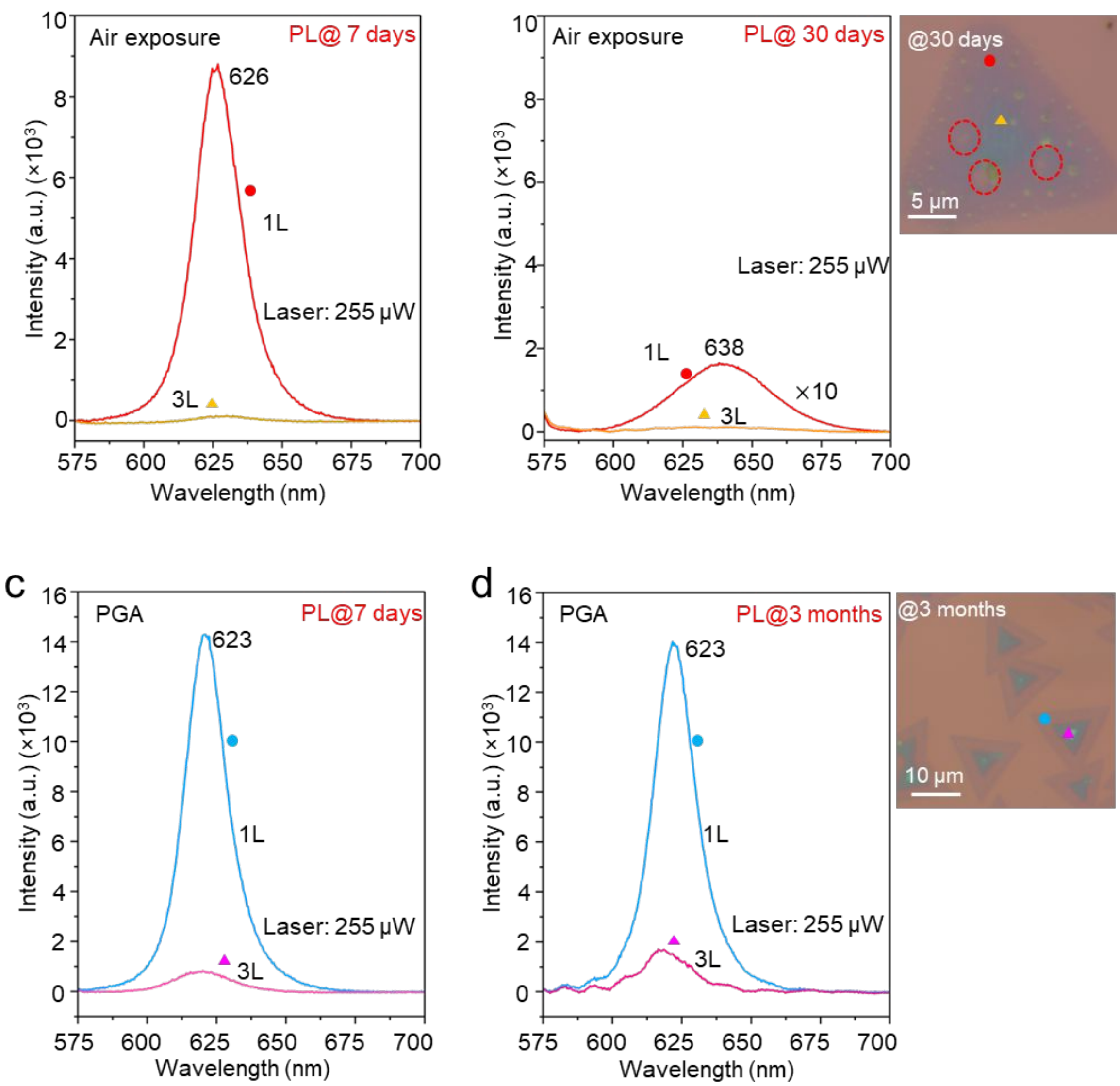

Figure S7. (a,b) PL spectra from representative 1L and 3L regions of an air-exposed as-grown NaCl-assisted WS_2 flake after 7 and 30 days, respectively, with corresponding the optical images. (c,d) PL spectra from representative 1L and 3L regions of a PGA-treated flake after 7 days and 3 months, respectively, with corresponding optical images.

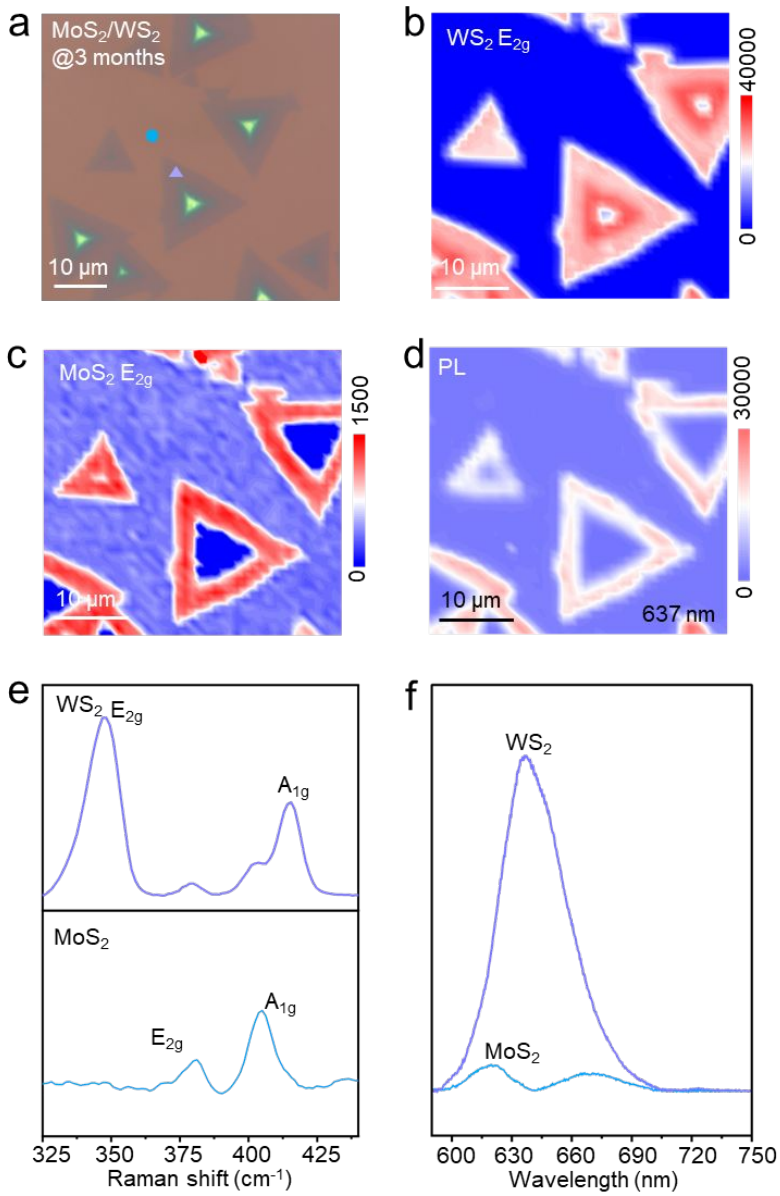

Figure S8. (a) OM image of representative MoS_2/WS_2 heterostructure flakes after 3 months of ambient storage. (b,c) Raman intensity maps of the WS_2 E_{2g} and MoS_2 E_{2g} modes. (d) PL intensity map at 637 nm. (e,f) Representative Raman and PL spectra from the marked positions in (a).

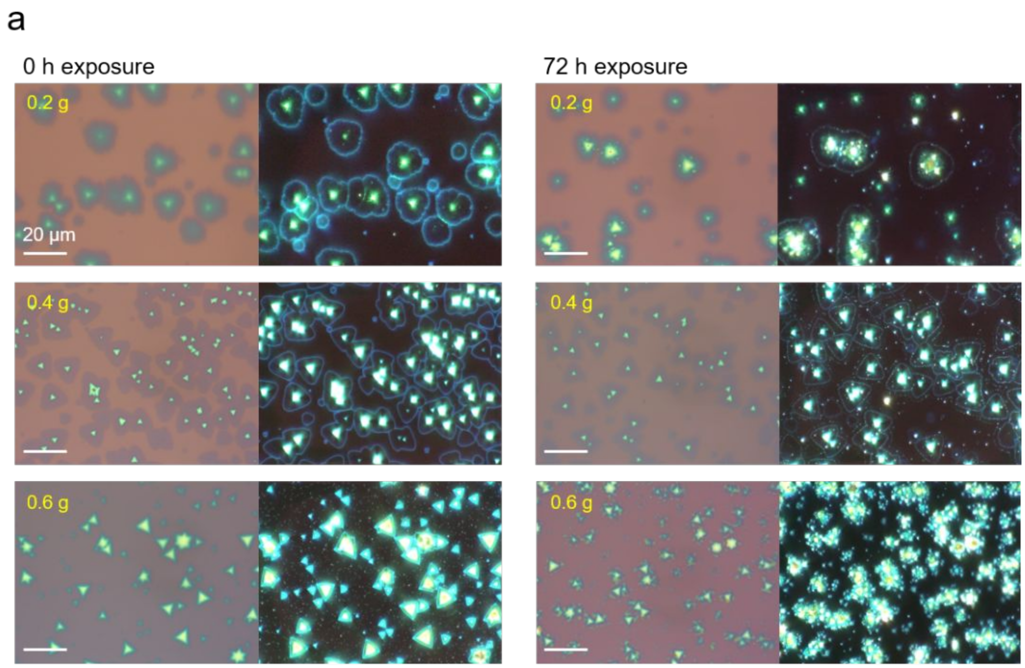

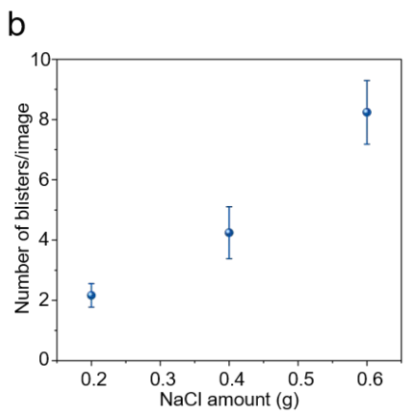

NaCl (g)	S1	S2	S3	S4	S5	S6	Mean	SD
0.2	184	198	216	254	272	175	216.5	39.0
0.4	446	345	375	340	486	555	424.5	86.2
0.6	655	878	954	776	792	889	824.0	105.8

S1-S6: Sample 1-6

Figure S9. Effect of NaCl loading on WS_2 growth morphology and residue-driven protrusion formation. (a) Bright-field and dark-field optical microscopy images of NaCl-assisted WS_2 grown with 0.2, 0.4, and 0.6 g NaCl before (0 h) and after (72 h) ambient air exposure. With increasing NaCl loading, flake morphology evolves from poorly defined, rounded domains (0.2 g) to well-defined triangular flakes (0.6 g), with correspondingly increased protrusion density in dark-field. (b) Protrusion density after 72 h exposure as a function of NaCl loading amount. Data points represent mean ± standard deviation (N = 6 independent image regions per condition; image area:

112 μm × 84 μm; blister count ×10^2 per image). Individual counts and summary statistics (mean ± SD) for all six regions are provided in the accompanying table.

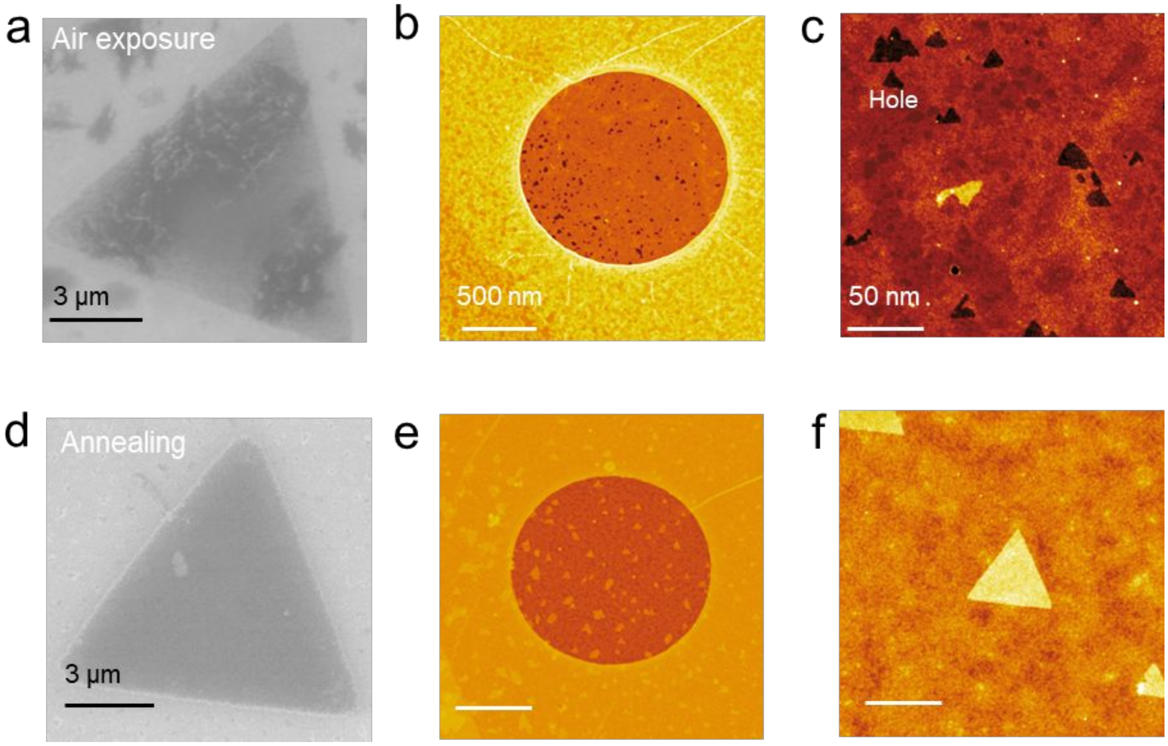

Figure S10. (a,d) SEM images of the air-exposed as-grown and PGA-treated samples, respectively. (b,c) STEM images of representative bilayer regions from the air-exposed sample. (e,f) STEM images of representative bilayer regions from the PGA-treated sample.

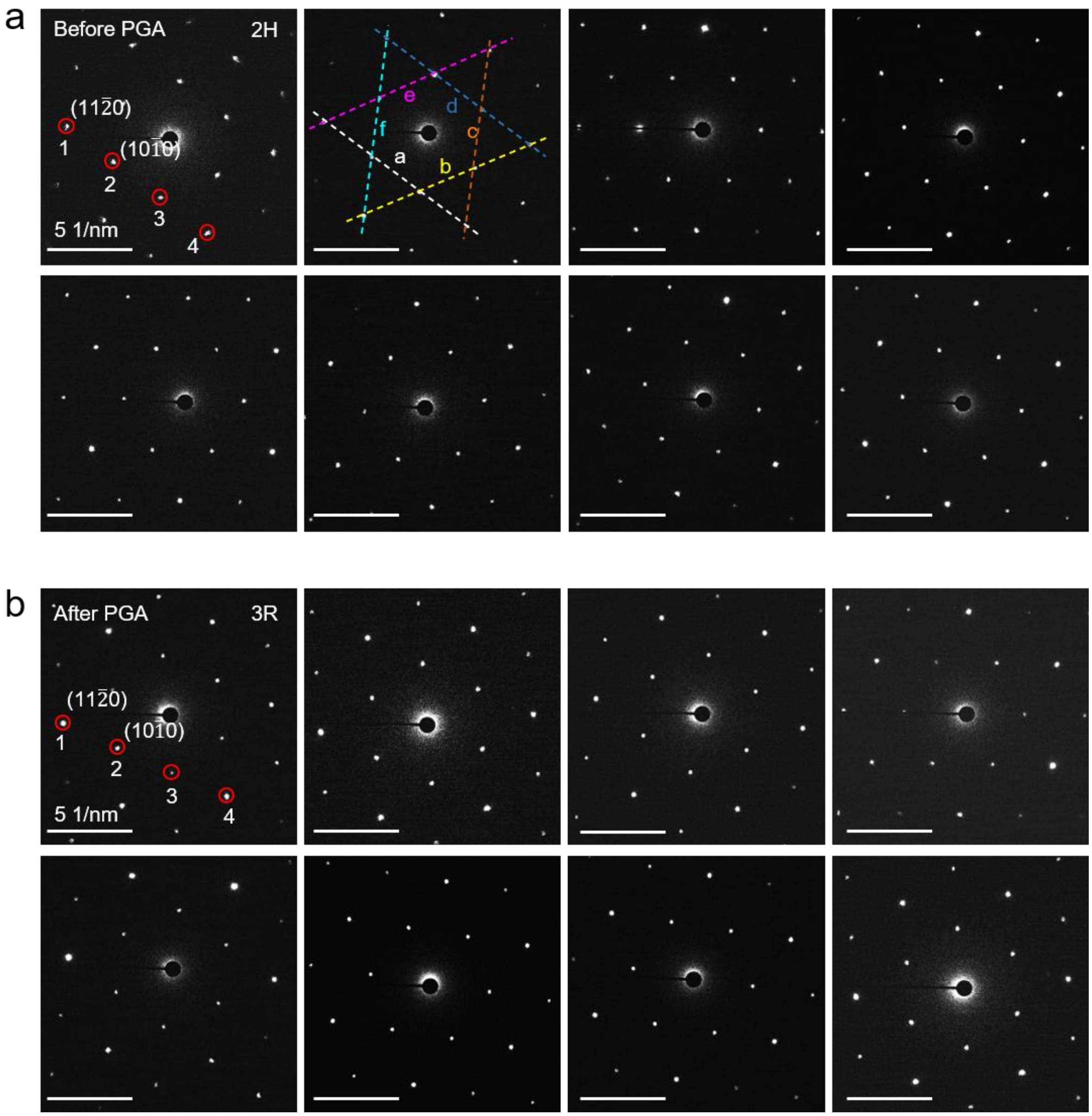

Figure S11. SAED patterns used for stacking-statistics analysis. (a, b) Representative SAED patterns collected from multilayer WS_2 regions before PGA (a) and after PGA (b). For each condition, N = 10 independent multilayer regions were analyzed; 8 representative patterns are shown here, with the remaining 2 presented in Figure 4 and Figure 5. For each pattern, the inner/outer diffraction-spot intensity ratio (I^{inner}/I^{outer}) was measured along six crystallographic line profiles, from two symmetry-equivalent spot pairs corresponding to the $\{10\bar{1}0\}$ and $\{11\bar{2}0\}$ reflections, and averaged into a single representative ratio per region.

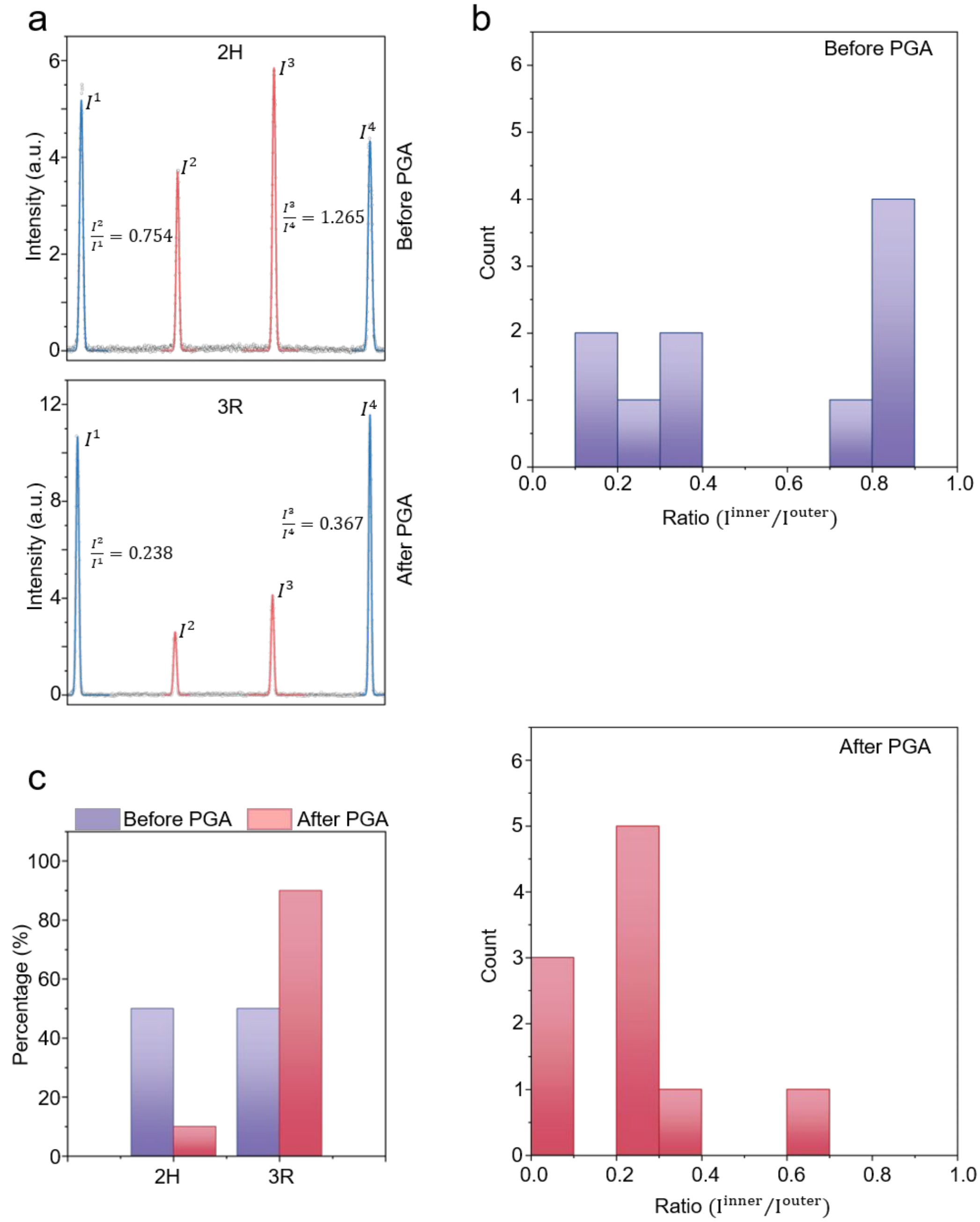

Figure S12. Statistical analysis of 2H and 3R stacking before and after PGA. (a) Representative spot-intensity profiles for 2H- and 3R-stacked bilayer WS_2. (b) Histograms of region-averaged I^{inner}/I^{outer} ratio (N =10 independent regions per condition) before and after PGA. (c) Percentage of 2H- and 3R-classified regions before and after PGA, based on the region-averaged ratios shown in (b), with each region classified as 3R (≤ 0.45) or 2H (> 0.45).

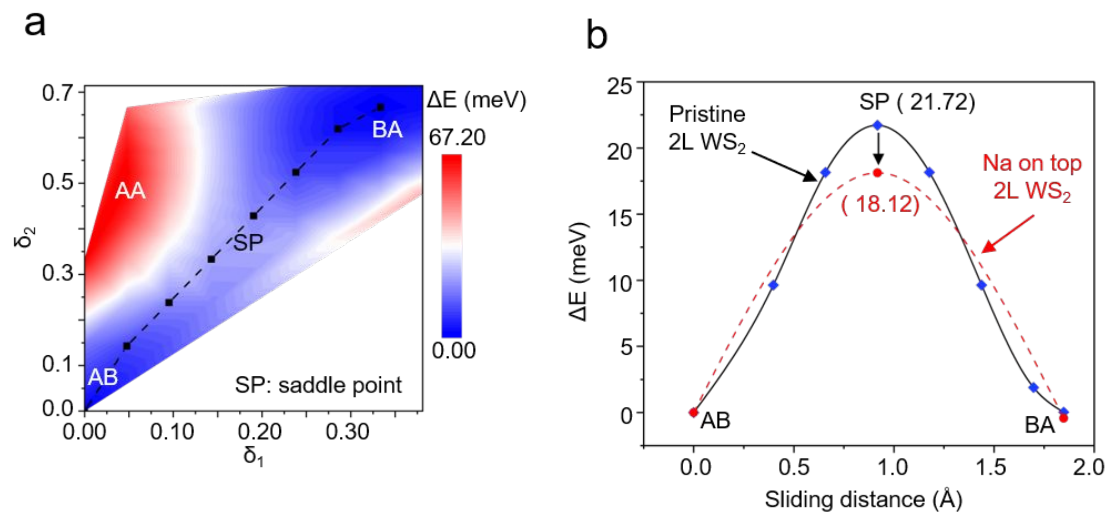

Figure S13. Generalized stacking fault energy (GSFE) analysis of interlayer sliding in bilayer WS_2. (a) Two-dimensional GSFE map computed over 62 displacement points on the primitive cell using a rigid-sliding protocol, covering the AB→BA sliding corridor; energies range from 0 meV at the AB and BA minima to ~67 meV at the boundary of the sampled region. The dashed line indicates the minimum-energy path connecting AB and BA through the saddle point (SP); the AA configuration (global maximum, 221 meV per unit cell) lies outside the sampled region. (b) One-dimensional GSFE profiles along the minimum-energy path for pristine bilayer WS_2 (black) and a 4×4 supercell with one Na atom adsorbed on the top WS_2 surface (red dashed). Surface Na reduces the interlayer sliding barrier from 21.72 meV (pristine) to 18.12 meV (~16% reduction).